COBEM 2023 27TH INTERNATIONAL CONGRESS OF MECHANICAL ENGENEERING

ABCM Brazilian Society of Mechanical Sciences and Engineering
27th ABCM International Congress of Mechanical Engineering
December 04-08, 2023, Florianópolis-SC, Brazil

COB-2023-2135
ANALYSIS OF NUCLEAR DESALINATION USING REJECTED AND EXTRACTED HEAT IN SMALL MODULAR REACTOR WITH MEMBRANE DISTILLATION

Gabriel C. G. R. da Silva
Nuclear Engineering Program, Federal University of Rio de Janeiro, COPPE/UFRJ, Rio de Janeiro, RJ, Brazil
gabriel.caetano@coppe.ufrj.br

Renato M. Cotta
Mechanical Engineering Program, Federal University of Rio de Janeiro, POLI & COPPE/UFRJ, Rio de Janeiro, RJ, Brazil
IPqM/ DGDNTM, General Directorate of Nuclear and Technological Development, Brazilian Navy, Rio de Janeiro, RJ, Brazil
cotta@mecanica.coppe.ufrj.br

Jian Su
Nuclear Engineering Program, Federal University of Rio de Janeiro, COPPE/UFRJ, Rio de Janeiro, RJ, Brazil
sujian@coppe.ufrj.br

Abstract. *Nuclear desalination has positioned itself as a reliable and cost-effective means of producing potable water, and small modular reactors (SMRs) are reportedly ideal for desalination purposes. This work investigated the thermal coupling of the NuScale reactor, a 50 MWe SMR, and a direct contact membrane distillation (DCMD) desalination plant with heat recovery and feed recycle. Both the waste heat and the low pressure (LP) steam extractions from the reactor turbine were assessed as energy sources for desalination. Longer DCMD modules presented higher values of gain to output ratio (GOR), indicating higher thermal efficiency and, thus, higher distilled water production. The LP steam extractions were not only capable of boosting the distilled water production of the desalination plant, but also highly reduced the total membrane area necessary for desalination. The proposed coupling schemes were able to produce up to 5,429 m^3/d of distilled water.*

Keywords: *Nuclear desalination, Membrane distillation, Waste heat recovery, Small modular reactors, DCMD*

1. INTRODUCTION

Due to the increasing depletion of water resources worldwide, desalination techniques are expected to play an important role in the near future (Voutchkov, 2018). Nuclear desalination plants are defined by the International Atomic Energy Agency (IAEA) as desalination facilities that use energy from a nuclear reactor. Along the past decades, nuclear desalination has shown to be a reliable and cost-effective solution for water desalination (Alonso *et al.*, 2012). Small modular reactors (SMRs), which are considered the future of nuclear energy, are reportedly ideal sources of energy for desalination (Alonso *et al.*, 2012; Ingersoll *et al.*, 2014). The most common technologies deployed in existing nuclear desalination facilities are: multi-stage flash (MSF), multi-effect distillation (MED), and reverse osmosis (RO). MSF and MED are highly energy-intensive thermal processes, while RO is a membrane technology, which is much less energy intensive, but produces a product with less quality when compared to MSF and MED. These technologies are often used combined for an optimized production (Alonso *et al.*, 2012).

One of the emerging desalination technologies is the membrane distillation (MD), which comprises the benefits of both thermal and membrane technologies. It consists of a separation process through a hydrophobic membrane, where the partial pressure gradient across the membrane due to temperature difference is the driving force for desalination. Since the water transport across the membrane pores is in the vapor phase, unlike in the RO, the distilled product of the MD presents high quality, similar to MSF and MED. The advantage of MD is its low sensitivity to the feed salinity and compatibility with low-grade heat sources, such as waste heat from nuclear reactors (Deshmukh *et al.*, 2018). The simplest and most utilized MD configuration is the direct contact membrane distillation (DCMD), where the hot feed solution is separated from the cold permeate by the membrane, which is commonly assembled in flat sheets or in hollow fibers.

Many works in literature have assessed the DCMD, both theoretically (Long *et al.*, 2018; Lisboa *et al.*, 2019, 2021; Sampaio, 2022a; Anjos *et al.*, 2022; Andrjesdottir *et al.*, 2013; Dutta *et al.*, 2020) and experimentally (Andrjesdottir *et al.*, 2013; Dutta *et al.*, 2020; Wang *et al.*, 2008; Yang *et al.*, 2011). Due to the their high energy-intensive nature, MD plants are ideally associated with heat recovery systems (Dutta *et al.*, 2020; Lisboa *et al.*, 2021; Sampaio, 2022a; Anjos *et al.*, 2022; Long *et al.*, 2018) and/or feed recycle (Andrjesdottir *et al.*, 2013; Dutta *et al.*, 2020; Sampaio, 2022a; Anjos *et al.*,

2022).

There are only a few works in literature regarding nuclear desalination via MD (Sampaio *et al.*, 2022b; Silva *et al.*, 2022; Sampaio *et al.*, 2023). In Silva *et al.* (2022), the direct thermal coupling of a DCMD plant with the NuScale reactor was investigated. NuScale is one of the most advanced SMR designs in the world, with an electrical output of 50 MWe per module. The proposed thermal coupling was capable of producing up to 2,000 m ^{3}/d of water using exclusively the reactor waste heat. Sampaio *et al.* (2022b) showed that the steam extraction from the low pressure turbine of a 25.4 MWe reactor was capable of producing 1,502 m^3/d of water via DCMD, with a reactor power loss of 0.61 MW. More recently, Sampaio *et al.* (2023) proposed the thermal coupling of a small PWR of 75MWt to a DCMD desalination plant with heat recovery. Two different coupling schemes were investigated: (i) using steam extractions from the reactor turbine and (ii) using two parallel Rankine cycles. The coupling scheme with parallel Rankine cycles was the one with the highest distilled water production, 7,577 m^3/d, at the expense of a reactor electrical output reduction of 2.53 MW.

The present work goes beyond the use of waste heat recovery from the low pressure steam of the turbine exhaust, presented in Silva *et al.* (2022), and explores the extraction of higher pressure steam for desalination, sacrificing part of the reactor electrical output. The objective is to assess the relative merits of utilizing part of the useful thermal energy towards increasing the distilled water production.

2. METHODOLOGY

The physical problem is the direct coupling of the secondary cooling system of the NuScale reactor with the desalination plant shown in Fig. 1. The desalination plant comprises a DCMD module, two recovery heat exchangers (each one recovering heat from one of the module outlet streams), a brine heater and a feed recycle, through which the feed outlet solution can be partially recycled in order to reduce the saline feed water consumption of the plant. The DCMD module is an assembly of hollow fiber permeators in parallel, where the two phases (permeate and feed) flow countercurrently.

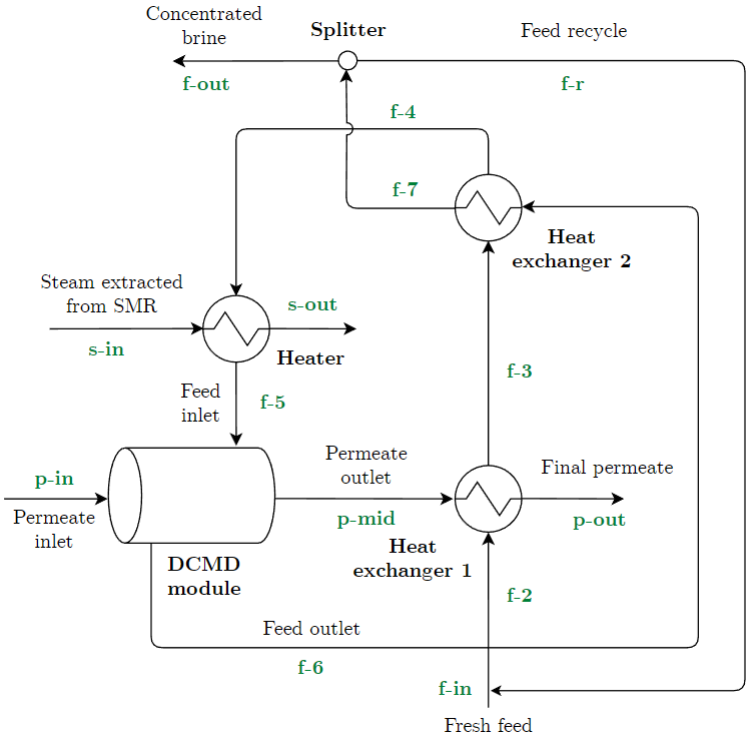

Figure 1. Flow diagram of the desalination plant.

The mathematical model comprises two parts: the permeator and the desalination plant. In both of them, steady-state and constant fluid thermophysical properties were assumed.

2.1 Permeator

The permeator was modeled as a porous medium where the two phases flow in countercurrent (Lisboa *et al.*, 2021). The feed flows in the shell side while the permeate flows in the hollow fibers.

The hydraulic diameters of the phases are:

$$D_{hp} = 2r_{fi} \ , \quad D_{hf} = \frac{2r_s^2\left(1 - N_{fbr}\left(\frac{r_{fe}}{r_s}\right)^2\right)}{N_{fbr}r_{fo}} \tag{1}$$

where N_{fbr} is the number of fibers in the porous medium representing a single permeator, r_{fi} and r_{fo} are the inner and outer radii of the fiber, respectively, and r_s is the radius of the shell. The subscripts p and f indicate the permeate and the feed phases, respectively.

The superficial velocities of the phases v_p and v_f are defined as:

$$v_p = \frac{Q_p}{\pi r_s^2} \ , \quad v_f = -\frac{Q_f}{\pi r_s^2} \tag{2}$$

where Q is the volumetric flow rate.

Assuming that the temperature profiles are independent of the radial coordinate, the energy conservation equations for each phase, with their respective boundary condition, can be written as (Lisboa *et al.*, 2021):

$$\begin{cases} \rho_p c_{pp} v_p \dfrac{\mathrm{d}T_p}{\mathrm{d}z} = -a_p h_p (T_p - T_{pm}) \\ T_p(0) = T_{ip} \end{cases} \ , \quad \begin{cases} \rho_f c_{pf} v_f \dfrac{\mathrm{d}T_f}{\mathrm{d}z} = -a_f h_f (T_f - T_{fm}) \\ T_f(L) = T_{if} \end{cases} \tag{3}$$

where h is the heat transfer coefficient, T_{ip} and T_{if} are the inlet temperatures of the permeate and the feed, respectively, T_{pm} and T_{fm} are the temperatures of the permeate and the feed phases at the membrane interface. The specific surface area a is defined as the ratio between the area available for heat transfer in each phase divided by the total volume of the porous medium:

$$a_p = \frac{2N_{fbr}r_{fi}}{r_s^2} \ , \quad a_f = \frac{2N_{fbr}r_{fo}}{r_s^2} \tag{4}$$

The heat transfer coefficient h of each phase was calculated by the following correlations (Sampaio, 2022a; Lisboa *et al.*, 2021):

$$\begin{cases} \dfrac{hD_h}{k} = 4.36 + \dfrac{0.036RePr(D_h/L)}{1 + 0.0011[RePr(D_h/L)]^{0.8}} \ , & Re < 2100 \\ \dfrac{hD_h}{k} = \dfrac{(Re - 1,000)Pr(f/8)}{1.07 + 12.7(Pr^{2/3} - 1)(f/8)^{1/2}} \ , & Re \geq 2100 \end{cases} \tag{5}$$

where Pr is the Prandtl number ($c_p\mu/k$) and Re is the Reynolds number ($uD_h\rho/\mu$), calculated from the actual velocity u of each phase. The friction factor f was calculated by (Sampaio, 2022a; Lisboa *et al.*, 2021):

$$f = [0.79\ln(Re) - 1.64]^{-2} \tag{6}$$

Assuming that the water flux $j_{w,r}$ is oriented inward the hollow fiber, the temperatures at the membrane interfaces can be calculated by the following algebraic expressions (Lisboa *et al.*, 2021):

$$T_{fm} = T_f - \left[1 + \frac{r_{fo}h_f(T_{fm} - T_{pm})\ln(r_{fo}/r_{fi})}{k_m(T_{fm} - T_{pm}) + j_{w,r}h_{lv}r_{fi}\ln(r_{fo}/r_{fi})} + \frac{r_{fo}h_f}{r_{fi}h_p}\right]^{-1}(T_f - T_p) \tag{7}$$

$$T_{pm} = T_p + \left[1 + \frac{r_{fi}h_p(T_{fm} - T_{pm})\ln(r_{fo}/r_{fi})}{k_m(T_{fm} - T_{pm}) + j_{w,r}h_{lv}r_{fi}\ln(r_{fo}/r_{fi})} + \frac{r_{fo}h_f}{r_{fi}h_p}\right]^{-1}(T_f - T_p) \tag{8}$$

The water flux $j_{w,r}$, which is measured at the membrane inner surface, can be estimated by the Dusty Gas Model, assuming that the membrane pores are filled with air, considering only ordinary and Knudsen diffusion. Disregarding the mass transfer resistance in both phases yields (Lisboa *et al.*, 2021):

$$j_{w,r} = \frac{M_w D^0_{wa}}{RT_m r_{fi} \ln(r_{fo}/r_{fi})} \ln\left(\frac{D^0_{wa} - p_p D_{eff}}{D^0_{wa} - p_f D_{eff}}\right) \tag{9}$$

where M_w is the molar mass of water, T_m is the average membrane temperature, R is the gas constant, p_p and p_f are the water partial pressures at both sides of the membrane (permeate and feed). D^0_{wa} is the ordinary diffusion coefficient of water vapor in air and D_{eff} is the effective diffusivity, defined as:

$$D_{eff} = \frac{D^k_w D^0_{wa}}{D^0_{wa} + pD^k_w} \tag{10}$$

The ordinary diffusion coefficient D^0_{wa} and the Knudsen diffusion coefficient D^k_w are calculated by (Andrjesdottir *et al.*, 2013; Lisboa *et al.*, 2021):

$$D^0_{wa} = 4.46 \times 10^{-6} \frac{\phi}{\tau_m} T_m^{2.334} \ , \quad D^k_w = \frac{\phi}{\tau_m} \frac{d_p}{3} \sqrt{\frac{8RT_m}{\pi M_w}} \tag{11}$$

where ϕ is the membrane porosity, τ_m is the membrane pore tortuosity $(1/\phi)$ and d_p is the average pore diameter.

The partial pressures at the membrane interfaces are calculated by the modified Raoult's law:

$$p_f = (1 - x_f)\alpha_f p_{v,f} \ , \quad p_p = (1 - x_p)\alpha_p p_{v,p} \tag{12}$$

where x is the molar fraction of salt in water. The activity coefficient α and the vapor pressure p_v are calculated by (Lisboa *et al.*, 2021; Andrjesdottir *et al.*, 2013; Stull, 1947):

$$\alpha = 1 - 0.5x - 10x^2 \ , \quad \log_{10} p_v = 4.6543 - \frac{1435.264}{T - 64.848} \tag{13}$$

The properties of pure water were obtained from NIST REFPROP v.7.0 and the properties of saline water were calculated by the empirical correlations from Sharqawy *et al.* (2012).

The solution for the permeator was obtained by solving iteratively the Eqs. 3, 7, 8 and 9. The convergence criteria adopted were mass and energy residuals smaller than 10^{-5}.

The permeator mean mass flux $\bar{j}_{w,r}$ was calculated by:

$$\bar{j}_{w,r} = \frac{1}{L} \int_0^L j_{w,r}(z) \mathrm{d}z \tag{14}$$

2.2 Desalination plant

An algorithm was developed to evaluate the entire plant after an initial value is set for the flow rate ($\dot{m}$), temperature (T), and salt mass fraction (w) of the recycled stream (feed recycle). The convergence criteria of the algorithm was that the residuals for these three variables were $< 10^{-5}$. The following equations represent the mass balance for water in the system:

$$\dot{m}_{feed-2} = \dot{m}_{f-in} + \dot{m}_{f-r} \tag{15}$$

where $\dot{m}_{f-in}$ is computed using the given definition of the recycle ratio R:

$$R = \frac{\dot{m}_{f-r}}{\dot{m}_{f-in}} \tag{16}$$

$$\dot{m}_{f-5} = \dot{m}_{f-4} = \dot{m}_{f-3} = \dot{m}_{f-2} \tag{17}$$

$$\dot{m}_{f-7} = \dot{m}_{f-6} = \dot{m}_{f-5} - \dot{m}_d \tag{18}$$

$$\dot{m}_{p-out} = \dot{m}_{p-mid} = \dot{m}_{p-in} + \dot{m}_d \tag{19}$$

where $\dot{m}_d$ is the distillate flow rate, defined as:

$$\dot{m}_d = N_{perm} N_{fbr} \cdot 2\pi r_{fi} L \bar{j}_{w,r} \tag{20}$$

and N_{perm} is the number of permeators in the DCMD module, calculated by:

$$N_{perm} = \frac{\dot{m}_{p-in}}{Q_p \rho_p} \tag{21}$$

where Q_p is the volumetric flow rate of the permeate phase in each permeator.

To determine the remaining independent variable, the feed and permeate flow rates are related to each other through the system's flow rate ratio (Q_f/Q_p), which is the ratio between the volumetric flow rates of the phases within the DCMD module:

$$\dot{m}_{f-5} = \frac{Q_f}{Q_p} \frac{\rho_f}{\rho_p} \dot{m}_{p-in} \tag{22}$$

The mass balance equations for the salt are:

$$w_{f-2} = \frac{\dot{m}_{f-in} w_{f-in} + \dot{m}_{f-r} w_{f-r}}{\dot{m}_{f-in} + \dot{m}_{f-r}} \tag{23}$$

$$w_{f-5} = w_{f-4} = w_{f-3} = w_{f-2} \tag{24}$$

$$w_{f-6} = \frac{\dot{m}_{f-5} w_{f-5}}{\dot{m}_{f-6}} \tag{25}$$

$$w_{f-out} = w_{f-r} = w_{f-7} = w_{f-6} \tag{26}$$

$$w_{p-out} = w_{p-mid} = \frac{\dot{m}_{p-in} w_{p-in}}{\dot{m}_{p-mid}} \tag{27}$$

Below, the energy balance equations are provided, beginning with the heat recovery rates at the two heat exchangers (q_{hx1} and q_{hx2}):

$$q_{hx1} = \begin{cases} \varepsilon_1 \cdot \min[\dot{m}_{f-2} c_{pf}, \dot{m}_{p-mid} c_{pp}](T_{f-2} - T_{p-mid}) \,, \, T_{f-2} < T_{p-mid} \\ 0 \,, \, T_{f-2} \geq T_{p-mid} \end{cases} \tag{28}$$

$$q_{hx2} = \begin{cases} \varepsilon_2 \cdot \min[\dot{m}_{f-6} c_{pf}, \dot{m}_{f-3} c_{pf}](T_{f-6} - T_{feed-3}) \,, \, T_{f-3} < T_{f-6} \\ 0 \,, \, T_{f-3} \geq T_{f-6} \end{cases} \tag{29}$$

where ε_1 and ε_2 are the effectivenesses of the heat exchangers 1 and 2, respectively.

In Eqs. 28 and 29, the temperature conditions are enforced to ensure the recovery of heat from the module outlet streams in the heat exchangers, rather than the reverse situation of cooling the feed prior to its entry into the DCMD module. In practice, this is equivalent to bypassing the heat exchanger if the heat recovery condition is not satisfied (q_{hx1} = 0 in Eq. 28 and q_{hx2} = 0 in equation 29).

The temperatures of all the streams are:

$$T_{f-in} = T_{p-in} = T_{ip} \tag{30}$$

$$T_{f-2} = \frac{\dot{m}_{f-in} T_{f-in} + \dot{m}_{f-r} T_{f-r}}{\dot{m}_{f-in} + \dot{m}_{f-r}} \tag{31}$$

$$T_{f-3} = T_{f-2} + \frac{q_{hx1}}{c_{pf} \dot{m}_{f-2}} \tag{32}$$

$$T_{f-4} = T_{f-3} + \frac{q_{hx2}}{c_{pp} \dot{m}_{f-3}} \tag{33}$$

$$T_{f-5} = T_{if} \tag{34}$$

$$T_{f-6} = T_f(0) \tag{35}$$

$$T_{f-7} = T_{f-6} - \frac{q_{hx2}}{c_{pf} \dot{m}_{f-6}} \tag{36}$$

$$T_{p-mid} = T_p(L) \tag{37}$$

$$T_{p-out} = T_{p-mid} - \frac{q_{hx1}}{c_{pp} \dot{m}_{p-mid}} \tag{38}$$

The heater duty q_h is:

$$q_h = \dot{m}_{f-4} c_{pf} (T_{if} - T_{f-in}) - q_{hx1} - q_{hx2} \tag{39}$$

The fraction of steam consumed in the heater F_s is calculated by:

$$F_s = \frac{q_h}{\dot{m}_{s-in} h_{lv}^s} \tag{40}$$

where h_{lv}^s is the condensation enthalpy of the steam extracted from the secondary system of the reactor.

In order to ensure the full utilization of steam, the permeate inlet flow rate ($\dot{m}_{p-in}$) is arbitrated, the whole plant is calculated and the fraction F_s output is stored. Then a new value of $\dot{m}_{p-in}$ is calculated by dividing the first $\dot{m}_{p-in}$ by F_s. The plant is then recalculated ensuring that F_s equals 1.00 and, thus, all the available steam is used in the heater.

The gain output ratio (GOR), which is a measure of the efficiency of the entire plant, is defined as:

$$GOR = \frac{\dot{m}_d h_{lv}^f}{q_h} \tag{41}$$

where h_{lv}^f is the vaporization enthalpy of the feed water.

Finally, the total production of the plant P is simply the distillate flow rate $\dot{m}_d$ expressed in m^3/d and the total membrane area A_m is calculated by:

$$A_m = N_{perm} N_{fbr} 2\pi \left(\frac{r_{fi} + r_{fo}}{2} \right) L \tag{42}$$

2.3 Turbine extraction

This work investigated two possibilities: (i) the desalination via waste heat recovery and (ii) the desalination with turbine extraction. The first considered exclusively the steam of the turbine exhaust (TE) while the latter considered the extraction of steam at one of the turbine extraction ports (for feedwater preheating in the secondary system). Considering that the extraction of high pressure steam for desalination generally results in higher reactor power loss per mass of produced water (Ingersoll *et al.*, 2014) and that the DCMD is a low-efficiency desalination technique, only the low pressure (LP) steam extraction was investigated. The properties of the steam in both cases is presented in Tab. 1 (NuScale Power, 2016).

Table 1. Properties of secondary system steam (NuScale Power, 2016).

Property	**Symbol**	**Unit**	**LP**	**TE**
Mass flow rate	$\dot{m}$	kg/s	50.9	50.9
Temperature	T	°C	86.8	41.7
Pressure	p	kPa	62.1	8.1
Enthalpy	h	kJ/kg	2,401.0	2,259.4
Condensation enthalpy	h_{lv}	kJ/kg	2,226.5	2,084.9

For the desalination with turbine extraction, both the total and partial extractions were considered. For the analysis of partial extractions, two separate DCMD plants were considered working in parallel, one using the low grade steam (TE) and the other, the low pressure (LP) steam extracted from the turbine.

The reactor power loss $\dot{W}_{lost}$ due to extraction was calculated by:

$$\dot{W}_{lost} = (h_{LP} - h_{TE})\dot{m}_{LP} \ , \tag{43}$$

where $\dot{m}_{LP}$ is the mass flow rate of medium pressure steam extracted from the turbine. Due to mass conservation in the turbine, the following relation was used for all the cases studied:

$$\dot{m}_{LP} + \dot{m}_{TE} = \ 50.9 \text{ kg/s} \tag{44}$$

The level of extraction was evaluated by the mass fraction of LP steam extracted from the turbine w_{LP}, defined as:

$$w_{LP} = \frac{\dot{m}_{LP}}{\dot{m}_{LP} + \dot{m}_{TE}} \tag{45}$$

3. RESULTS

The permeator model utilized in this work was capable of providing accurate water flux predictions for different experimental modules within a wide range of feed inlet temperatures, as presented in Silva *et al.* (2022).

The permeator parameters utilized were based on the work of Yang *et al.* (2011) and are presented in Tab. 2. An enhanced commercial membrane was considered in this study, with a slightly higher membrane porosity and lower polymer thermal conductivity, compared to the membrane used in Yang *et al.* (2011). The feed inlet temperature was assumed 40ºC for the waste heat application and 85ºC for the LP extraction, considering a minimum temperature difference of around 1.8 ºC in the feed heater (Fig. 1), where the steam presented in Tab. 1 gets condensed. The permeator length L and the feed inlet flow rate Q_f were considered as independent parameters. The additional parameters used for closure of the plant were: the recycle ratio R = 100, the heat recovery effectiveness, which was assumed to be ε = 0.75 for both heat exchangers, and the steam data from Tab. 1.

In Fig. 2, the GOR is presented as a function of the flow rate ratio Q_f/Q_p for the waste heat recovery plant (Fig. 2a) and for the plant with steam extraction (Fig. 2b). It was observed that, in both plants, the GOR and, consequently, the distilled water total production, reached a maximum for the largest module length studied (900 mm), for a flow rate ratio $Q_f/Q_p \approx 1$. This happens because, in longer modules operating at lower flow rate ratios, the heat is recovered exclusively from the permeate outlet (q_{hx2}=0), whereas, in shorter modules, the heat is recovered exclusively from the feed outlet (q_{hx1}=0), which is already accomplished by the feed recycle, present in all modules.

In Tab. 3, different coupling schemes are presented considering the module length L = 900 mm and the flow rate ratio Q_f/Q_p = 1.0, which corresponds to the maximum GOR in both the waste heat plant and in the plant with steam extraction (Fig. 2). In Tab. 3, the coupling 1 corresponds to the waste heat desalination plant, while coupling 5 corresponds to the desalination plant with total LP steam extraction. Couplings 2, 3 and 4 correspond to desalination plants with partial

Table 2. DCMD module parameters.

Parameter	**Symbol**	**Value**	**Unit**
Hollow fiber inner radius	r_{fi}	0.49	mm
Permeator shell inner radius	r_s	9.50	mm
Membrane thickness	δ	235	μm
Permeator length	L	variable	mm
Number of fibers	N_{fbr}	51	-
Membrane porosity	ϕ	0.90	-
Membrane pore diameter	d_p	0.164	μm
Membrane polymer thermal conductivity	k_{pl}	0.20	W/m·K
Feed inlet volumetric flow rate	Q_f	variable	l/s
Permeate inlet volumetric flow rate	Q_p	0.4	l/s
Feed inlet temperature	T_{if}	variable	°C
Permeate inlet temperature	T_{ip}	24.85	°C
Salt mass fraction in feed	w_f	0.035	-
Salt mass fraction in permeate	w_p	0.000	-
Operation pressure	p	101,325	Pa

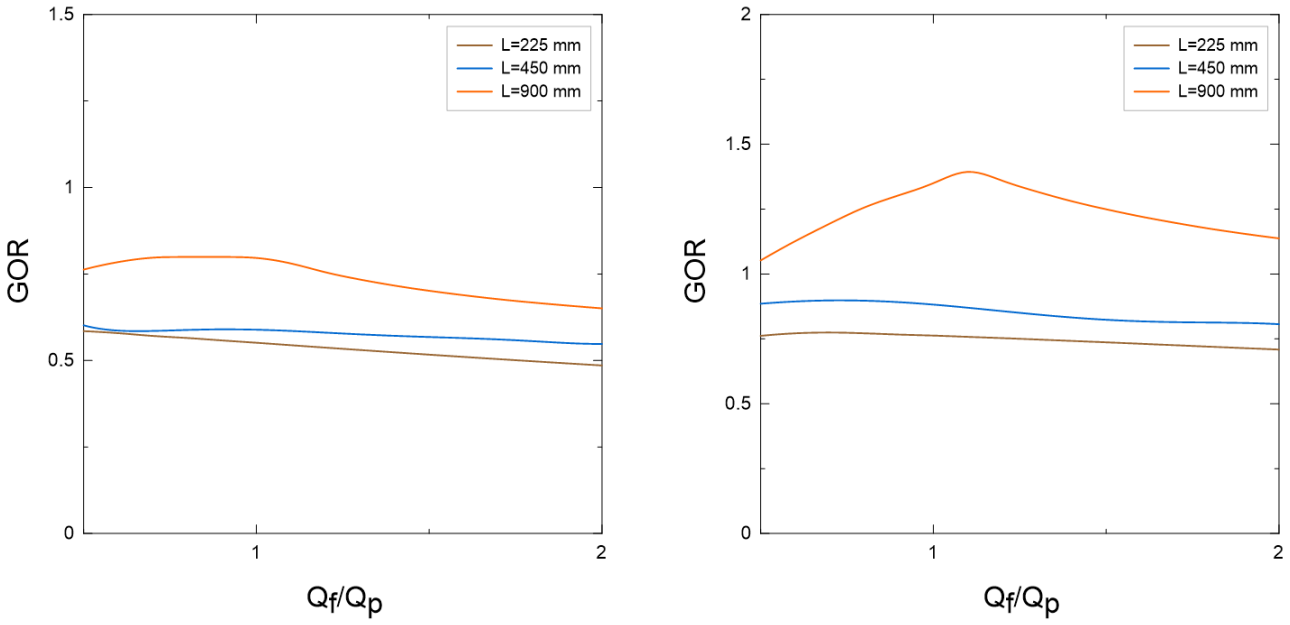

(a) (b)

Figure 2. GOR as a function of the flow rate ratio Q_f/Q_p for (a) the waste heat recovery plant and (b) the desalination plant with LP steam extraction.

LP steam extraction, with different levels of extraction (w_{LP} = 25, 50 and 75%, respectively). It was observed that the extraction of LP steam not only increased the distilled water production, but also greatly reduced the total membrane area demanded by the DCMD module.

The reactor electrical output W_e is presented in Fig. 3 as a function of the total distilled water production P for different levels of extraction. The gray points represent the levels of LP steam extraction (0, 25, 50, 75 and 100%). The blue and orange lines correspond to the desalination plants proposed by Ingersoll *et al.* (2014) for the same reactor, considering the MED and MSF desalination technologies, respectively, associated with medium pressure (MP) steam extractions. It can be seen that, for lower levels of distilled water production (up to approximately 3,500 m^3/d), the coupling with DCMD may compete with the referenced thermal desalination technologies, providing distilled water with reduced impact on the reactor electricity output.

Table 3. Different coupling schemes studied.

Coupling	1	2	3	4	5
$w_{LP}(\%)$	0	25	50	75	100
L **(mm)**	900	900	900	900	900
Q_f/Q_p	1.0	1.0	1.0	1.0	1.0
GOR	0.80	0.94	1.08	1.21	1.35
P **(m^3/d)**	3,095.9	3,679.2	4,262.5	4,845.8	5,429.1
A_m **(m^2)**	101,584.0	83,354.5	65,125.0	46,895.5	28,666.0
$\dot{W}_{lost}$ **(MWe)**	0.0	1.9	3.8	5.7	7.6
SEC (MWeh/m^3)	0.0	12.4	21.4	28.2	33.6

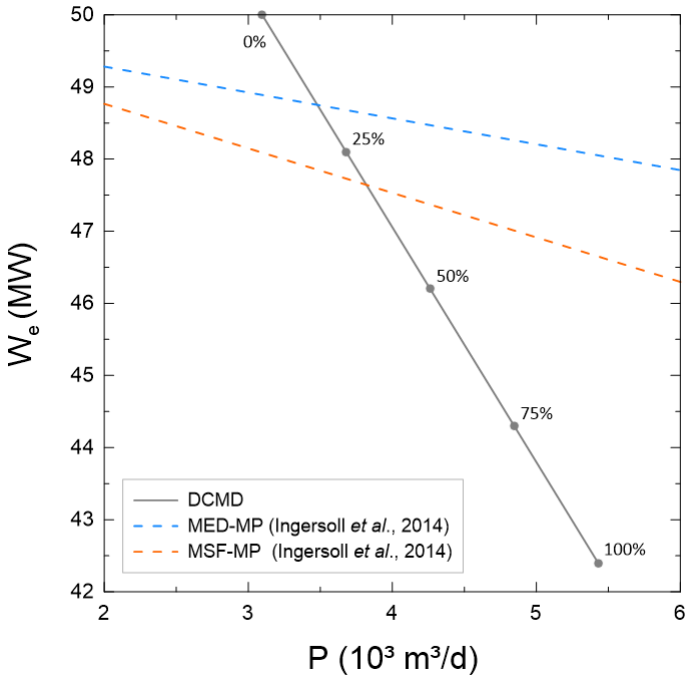

Figure 3. Reactor electrical output W_e as a function of the total distilled water production P for different levels of extraction in comparison with other desalination technologies.

4. CONCLUSIONS AND FUTURE IMPLEMENTATIONS

The thermal coupling between the NuScale reactor and a DCMD desalination plant was investigated considering both the waste heat recovery application and the desalination via low pressure (LP) steam extractions from the reactor turbine. The proposed coupling schemes were able to produce up to 5,429.1 m^3/d of distilled water. The extraction of LP steam not only increased the total water production of the DCMD plant but also greatly decreased the total membrane area required for desalination.

Despite the promising results, future implementations are projected to further increase the water production of the

proposed coupling, such as the utilization of higher performance membranes, multistage MD modules and alternative membrane distillation configurations, such as air-gap membrane distillation (AGMD) and vacuum membrane distillation (VMD).

5. ACKNOWLEDGEMENTS

The authors are thankful for the financial support provided by CAPES, CNPq and FAPERJ.

6. REFERENCES

Alonso, G., Vargas, S., Valle, E.D. and Ramirez, R., 2012. "Alternatives of seawater desalination using nuclear power". *Nuclear Engineering and Design*, Vol. 245, pp. 39–48.

Andrjesdottir, O., Ong, C.L., Nabavi, M., Paredes, S., Khalil, A.S., Michel, B. and Poulikakos, D., 2013. "An experimentally optimized model for heat and mass transfer in direct contact membrane distillation". *International Journal of Heat and Mass Transfer*, Vol. 66, pp. 855–867.

Anjos, E.B., Gomez, A.O.C., Chenche, L.E.P., Lima, J.A., Naveira-Cotta, C.P., Cotta, R.M. and Lisboa, K.M., 2022. "Enhancing DCMD efficiency for desalination at module scale through dua heat recovery and retentate recirculation". In *Proceedings of CONV-22: Int. Symp. on Convective Heat and Mass Transfer*. Izmir, Turkey, pp. 533–540.

Deshmukh, A., Boo, C., Karanikola, V., Lin, S., Straub, A.P., Tong, T., Warsinger, D.M. and Elimelech, M., 2018. "Membrane distillation at the water-energy nexus: limits, opportunities, and challenges". *Energy Environmental Science*, Vol. 11, pp. 1177–1196.

Dutta, N., Singh, B., Subbiah, S. and Muthukumar, P., 2020. "Performance analysis of a single and multi-staged direct contact membrane distillation module integrated with heat recovery units". *Chemical Engineering Journal Advances*, Vol. 4, 100055.

Ingersoll, D.T., Houghton, Z.J., Bromm, R. and Desportes, C., 2014. "NuScale small modular reactor for Co-generation of electricity and water". *Desalination*, Vol. 340, pp. 84–93.

Lisboa, K.M., de Moraes, D.B., Naveira-Cotta, C.P. and Cotta, R.M., 2021. "Analysis of the membrane effects on the energy efficiency of water desalination in a direct contact membrane distillation (DCMD) system with heat recovery". *Applied Thermal Engineering*, Vol. 182, 115769.

Lisboa, K.M., de Souza, J.R.B., Naveira-Cotta, C.P. and Cotta, R.M., 2019. "Heat and mass transfer in hollow-fiber modules for direct contact membrane distillation: Integral transforms solution and parametric analysis". *International Communications in Heat and Mass Transfer*, Vol. 109, 104373.

Long, R., Lai, X., Liu, Z. and Liu, W., 2018. "Direct contact membrane distillation system for waste heat recovery: Modelling and multi-objective optimization". *Energy*, Vol. 148, pp. 1060–1068.

NuScale Power, 2016. "NuScale Standard Plant Design Certification Application".

Sampaio, P.A.B., 2022a. "Computational model and simulation of DCMD desalination systems with heat recovery". *Desalination*, Vol. 533, 115769.

Sampaio, P.A.B., Alves, L.F.R. and Moreira, M.L., 2022b. "Cogeneration of electricity and water using a small PWR of 75 MW(th) coupled to a DCMD desalination system with heat recovery". In *Proceedings of the 19th Brazilian Congress of Thermal Sciences and Engineering - ENCIT 2022*. Bento Gonçalves, RS - Brazil.

Sampaio, P.A.B., Alves, L.F.R. and Moreira, M.L., 2023. "Electricity and water cogeneration using a small PWR of 75 MW(th) coupled to a DCMD desalination plant with heat recovery". *Nuclear Engineering and Design*, Vol. 415, 112658.

Sharqawy, M.H., V, J.H.L. and Zubair, S.M., 2012. "Thermophysical properties of seawater: a review of existing correlations and data". *Desalination and Water Treatment*, Vol. 16, pp. 354–380.

Silva, G.C.G.R., Lisboa, K.M., Su, J., Naveira-Cotta, C.P. and Cotta, R.M., 2022. "Assessment of desalination via membrane distillation using low-grade waste heat in small modular reactors". In *Proceedings of the 19th Brazilian Congress of Thermal Sciences and Engineering - ENCIT 2022*. Bento Gonçalves, RS - Brazil.

Stull, D.R., 1947. "Vapor pressure of pure substances. organic and inorganic compounds". *Industrial Engineering Chemistry*, Vol. 39, pp. 517–540.

Voutchkov, N., 2018. "Energy use for membrane seawater desalination – current status and trends". *Desalination*, Vol. 431, pp. 2–14.

Wang, K.Y., Chung, T.S. and Gryta, M., 2008. "Hydrophobic PVDF hollow fiber membranes with narrow pore size distribution and ultra-thin skin for the fresh water production through membrane distillation". *Chemical Engineering Science*, Vol. 63, pp. 2587–2594.

Yang, X., Wang, R. and Fane, A.G., 2011. "Novel designs for improving the performance of hollow fiber membrane distillation modules". *Journal of Membrane Science*, Vol. 384, pp. 52–62.

7. RESPONSIBILITY NOTICE

The authors are solely responsible for the printed material included in this paper.